Springer

Journal of
Mechanical
Science and
Technology

Journal of Mechanical Science and Technology 23 (2009) 3302~3315

www.springerlink.com/content/1738-494x
DOI 10.1007/s12206-009-1004-1

# A nonlinear model of flow-structure interaction between steam leakage through labyrinth seal and the whirling rotor †

W. Z. Wang[1], Y. Z. Liu[1,*], G. Meng[2] and P. N. Jiang[3]

[1]*Key Lab of Education Ministry for Power Machinery and Engineering, Shanghai Jiao Tong University, 800 Dongchuan Road, Shanghai 200240, China*

[2]*State Key Lab of Mechanical System and Vibration, Shanghai Jiao Tong University, 800 Dongchuan Road, Shanghai 200240, China*

[3]*Department of R&D, Shanghai Turbine Company, 333 Jiang Chuan Road, Shanghai 200240, China*

(Manuscript Received March 28, 2009; Revised August 13, 2009; Accepted August 21, 2009)

**Abstract**

A nonlinear model of flow-structure interaction between steam leakage through labyrinth seal and the whirling rotor was presented. The particular concern was placed on incorporating thermal properties of the steam fluid into the mathematical model. To see the influence of the steam fluid on the whirling rotor, two sets of thermal parameters of the steam fluid, e.g., temperature and pressure drop in each seal cavity, were selected from the typical 1000 MW supercritical and 300 MW subcritical power units in China. The interlocking seal widely employed in practical situations was chosen for study. The rotor-seal system was modeled as a Jeffcott rotor subject to shear stress and pressure force associated with the steam leakage. Spatio-temporal variation of the steam forcing on the rotor surface in the coverage of the seal clearance and the cavity volume was specifically delineated by using the Muzynska model and the perturbation analysis, respectively. The governing equation of rotor dynamics including the influence of the steam leakage was solved by using the fourth-order Runge-Kutta method, resulting in the orbit of the whirling rotor. Stability of the rotor was inspected by using Liapunov's first method. The results showed that the destabilization speed of the rotor was significantly influenced by the steam leakage.

***Keywords*:** Steam leakage; Nonlinear analysis; Leakage steam; Labyrinth seal; Muzynska model; Perturbation analysis

## 1. Introduction

Supercritical steam turbines have been widely established to meet the ever-increasing demand for thermal power in Asian countries. In the last decade, thermal efficiency of the units was enhanced by increasing the temperature and pressure of the steam fluid. However, the steam leakage through the labyrinth seals, which are placed between the rotor and the stator, would have a significant influence on the whirling rotor. With increasing temperature and pressure of the steam fluid, the flow-structure interaction between the rotor and the steam leakage may exhibit nonlinear behavior. Accordingly, a model for predicting the nonlinear behavior of the fluid-structure interaction between the steam leakage and the whirling rotor is highly desirable.

Various efforts have been attempted to numerically study the influence of the leakage flow through labyrinth seal on the whirling rotor. Through perturbation analysis [1-4], Kostyuk [5] and Iwatsubo [6] presented a linearized force-displacement model to see the aerodynamic influence of the leakage air flow on the rotordynamics. Subsequently, the rotordynamics coefficients associated with the leakage air flow through various labyrinth seals were numerically

† This paper was recommended for publication in revised form by Associate Editor Eung-Soo Shin

*Corresponding author. Tel.: +86 21 34206719, Fax.: +86 21 34206719
E-mail address: yzliu@sjtu.edu.cn

determined, e.g., the straight-through seal [1, 2, 7 and 8], the stepped seal [3, 4] and the honeycomb seal [9]. The unsteady static pressure in cavities of the interlock seal, which was numerically calculated by employing perturbation analysis, was demonstrated to be in favorable agreement with experimental measurements by Liu *et al.*[10]. The above-mentioned linear model was reduced from a preconditioned track of the whirling rotor, which slightly deviates from the statically balanced position; otherwise, the nonlinear behaviors of the whirling rotor, e.g., lock-on frequency and kick amplitude, could not be accurately captured by the linearized force-displacement model [2-4, 9-11]. Hua et al. [12] and Cheng et al. [13] carried out nonlinear analysis of the rotordynamics associated with leakage air flow through a simple annular seal by using the Muzynska model [14]. The authors [15] delineated the nonlinear behavior of the whirling rotor subjected to the leakage air flow through the labyrinth seal by using both perturbation analysis and Muzynska model. However, as for the steam leakage through the labyrinth seal, variation of the thermal parameters along the labyrinth seals is characterized by the isenthalpic process, resulting in the non-isothermal flow[16]. Steam properties, such as viscosity, density, enthalpy and local acoustic velocity, are governed by the IAPWS-IF97 formula [17] instead of the perfect gas law. Recently, the authors [11] constructed a linear model for calculating the rotordynamics coefficients associated with the steam leakage, in which particular concern was placed on incorporation of thermal properties of the steam fluid into the model. The comparative analysis based on assumptions of the IAPWS-IF97 and the perfect gas low demonstrated significantly different results of the whirling motion of the rotor associated with the steam leakage, indicating the essential influence of thermal properties of the steam fluid. However, a literature survey discloses that few studies on nonlinear influence of the steam leakage through labyrinth seal on the whirling rotor were reported.

As an extension of the authors' work [11, 15], a nonlinear model of the fluid-structure interaction between the steam leakage through a labyrinth seal and the rotor was established by considering the thermal properties of the steam fluid in terms of the specific IAPWS-IF97 [17]. The interlocking seal as shown in Fig. 1 was chosen for study. In calculations, the nonlinear steam forcing on the rotor surface in the coverage of the seal clearance and the cavity volume was reduced by using the Muzynska model and perturbation analysis, respectively [15]. For the comparative study, two sets of thermal parameters of the steam fluid, temperature and pressure drop in each seal cavity, were selected from the typical 1000 MW supercritical and 300 MW subcritical power units in China. The influence of the steam leakage through the interlocking seal on the whirling motion of the rotor was elaborated in terms of the rotating speed and inlet pressure. Stability of the whirling rotor was analyzed using Liapunov's first method.

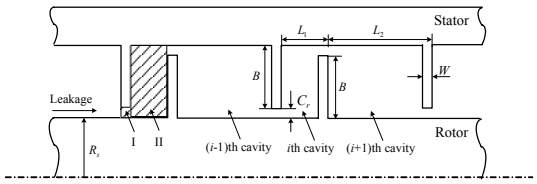


Fig. 1. Schematic diagram of the interlocking seal.

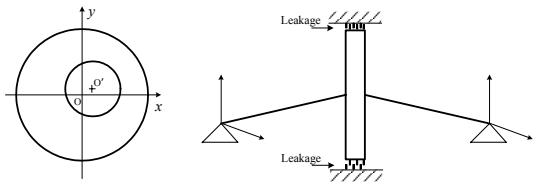


Fig. 2. Illustration of Jeffcott rotor system subject to leakage flow through the interlocking seal.

## 2. Mathematical model

In the present study, the Muzynska model and perturbation analysis were employed to determine the steam forcing on the rotor surface in the axial coverage of the seal clearances (zone I in Fig. 1) and of the cavity volumes (zone II in Fig. 1), respectively. Steam properties, e.g., viscosity, density, enthalpy and local acoustic velocity, are specified using IAPWS-IF97 formula [17]. As shown in Fig. 2, the rotor-seal system can be modeled as a Jeffcott rotor subject to aerodynamic forcing induced by the steam leakage. For ease of understanding the mathematical fundamentals of the nonlinear model, the full-length information regarding calculation of the steam leakage, steam forcing on the rotor surface [2, 11], governing equation of the rotor dynamics [11] and stability analysis [15] are hereafter presented.

### *2.1 Calculation of the steam leakage*

The serpentine geometry of the interlocking seal

Table 1. Dimension of the interlocking seal (mm).

| | | | |
|---|---|---|---|
| $L_1$ | 3 | B | 2.3 |
| $L_2$ | 7 | $C_r$ | 0.7 |
| W | 0.3 | $R_s$ | 50 |

placed between the stator and the rotor is illustrated in Fig. 1. Detailed information regarding its dimension can be found in Table 1. When the concentric rotor rotates at a constant speed, the air flow through the labyrinth seal is steady and axisymmetric. Thus, the continuity equation implies that the mass flow $m_i$ through the orifice between the seal tooth and the rotor is constant as $i$ varies from 1 to $N$ [2-4],

$$m_1 = m_2 = \cdots = m_i = \cdots = m_N = m_0 = C_0 C_1 A_0 \sqrt{2(P_{0i-1} - P_{0i})\rho_{0iseal}}, \quad (1)$$

where $m_0$ is the steady-state leakage flow rate. The steam flow is taken to be uniformly distributed and expanded isenthalpically [18] from cavity (*i*-1) to cavity (*i*). Detailed formulas of $C_0$ and $C_1$ are referred to the work [19]. When the critical condition appears at the last seal clearance, prediction of leakage steam flow [18] is determined by

$$m_0 = 0.647 C_0 A_0 \sqrt{P_{0N-1}\rho_{0N-1}}\ . \quad (2)$$

The isenthalpical process of steam flow through the labyrinth seal can be described by

$$h_{0iseal} + \frac{1}{2}U_{0iseal}^2 = h_0, \quad (3)$$

where $h_{0iseal}$ and $U_{0iseal}$ are the local enthalpy and the steam velocity at the *i*th orifice, respectively. Therefore, the temperatures in the *i*th cavity ( $T_i$ ) and at the *i*th orifice ( $T_{iseal}$ ) can be calculated by $T_{iseal} = f(P_{0iseal}, h_{0iseal})$ and $T_i = f(P_{0i}, h_0)$ specified by the IAPWS-IF97 formula. Furthermore, density of the steam at the *i*th orifice can be obtained by $\rho_{0iseal} = f(P_{0iseal}, T_{iseal})$. Wherein, the pressure $P_{0iseal}$ at the *i*th tooth clearance is averaged by the pressures in the two adjacent cavities,

$$P_{0iseal} = \frac{P_{0i-1} + P_{0i}}{2}\ . \quad (4)$$

Accordingly, the axial velocity at the clearance of the *i*th tooth is defined as

$$U_{0iseal} = \frac{m_{0i}}{A_0 \rho_{0iseal}}\ . \quad (5)$$

In addition, the circumferential steam flow induced by rotation of the rotor varies as the steam fluid consecutively flows along the cavities. The steady circumferential velocity $V_{0i}$ is governed by the momentum equation,

$$m_0(V_{0i} - V_{0i-1}) = \tau_{r0i}\pi R_s \alpha_r L - \tau_{s0i}\pi R_s \alpha_s L\ , \quad (6)$$

in which the shear stress terms $\tau_{r0i}$ and $\tau_{s0i}$ were empirically estimated by Dursun [2].

To solve the above system of equations, an iterative procedure is employed to calculate leakage flow rate, pressure distribution, temperature distribution, velocity distribution, circumferential velocity distribution and shear stresses in each seal cavity and orifice.

### *2.2 Steam forcing on the rotor surface in the coverage of the cavity volume*

In practice, the inherent whirling motion of the rotor implies that variables of the leakage flow, e.g., pressure, the circumferential velocity and shear stress, are actually non-uniform in the circumferential direction. When considering the fact that the seal clearance (zone I in Fig. 1) is considerably smaller than the cavity depth (zone II in Fig. 1), the flow variables in the cavity volume would hold a weakly nonlinear relationship with the whirling rotor; these fluctuating variables are then dealt with by using perturbation analysis. As an example, the dependence of the circumferential velocity of the steam fluid in the cavity volume on the time $t$ and the azimuthal position $\theta$ is obtained by solving the partial differential continuity and circumferential momentum equations,

$$\frac{\partial}{\partial t}(\rho_i A_n) + \frac{\rho_i V_i}{R_s}\frac{\partial A_n}{\partial \theta} + \frac{\rho_i A_n}{R_s}\frac{\partial V_i}{\partial \theta} + \frac{V_i A_n}{R_s}\frac{\partial \rho_i}{\partial \theta} + \dot{q}_{i+1} - \dot{q}_i = 0 \quad (7)$$

$$\rho_i A_n \frac{\partial V_i}{\partial t} + \frac{\rho_i V_i A_n}{R_s}\frac{\partial V_i}{\partial \theta} + (V_i - V_{i-1})\dot{q}_i = -\frac{A_n}{R_s}\frac{\partial P_i}{\partial \theta} + (\tau_{ri} a_r - \tau_{si} a_s)L. \quad (8)$$

The shear stresses at the rotor and stator walls are defined as Eqs. (9) and (10) by using Blasius formula,

$$\tau_{ri} = -0.03955\rho_i\left(V_i - R_s\omega\pi/30\right)^2\left(\frac{|V_i - R_s\omega|Dh}{\nu}\right)^{-0.25} \operatorname{sgn}\left(V_i - R_s\omega\pi/30\right), \quad (9)$$

$$\tau_{si} = 0.03955\rho_i V_i^2\left(\frac{|V_i|Dh}{\nu}\right)^{-0.25} \operatorname{sgn}\left(V_i\right). \quad (10)$$

Further linearization of Eqs. (7-10) is accomplished by using perturbation analysis. The perturbation parameter is defined as $\varepsilon = e/\left(C_r + B\right)$ for the cavity volume, where $e$ is a displacement of the rotor from the central position. The spatio-temporal variation of the radial clearance, which is caused by the whirling motion of the rotor, is expanded in the form of $H = C_r + \varepsilon H_1(t,\theta)$ . Accordingly, the seal cavity cross-sectional area $A$ and the flow variables can be expanded similarly. Substituting these linearized variables into Eq. (1) and neglecting the terms of order $\varepsilon^2$ and the higher, we obtain,

$$\dot{q}_{01} = \dot{q}_{02} = \cdots = \dot{q}_{0i} = \cdots = \dot{q}_0 = C_0 C_1 C_r\sqrt{2(P_{0i-1} - P_{0i})\rho_{0iseal}}, \quad (11)$$

and

$$\dot{q}_{1i} = \dot{q}_0\left[0.5\left(\frac{1}{P_{0i-1} - P_{0i}} + \frac{1}{2RT_{iseal}\rho_{0iseal}}\right)P_{1i-1} - 0.5\left(\frac{1}{P_{0i-1} - P_{0i}} - \frac{1}{2RT_{iseal}\rho_{0iseal}}\right)P_{1i} + \frac{H_1}{C_r}\right], \quad (12)$$

$$\dot{q}_{1i+1} = \dot{q}_0\left[0.5\left(\frac{1}{P_{0i} - P_{0i+1}} + \frac{1}{2RT_{i+1seal}\rho_{0i+1seal}}\right)P_{1i} - 0.5\left(\frac{1}{P_{0i} - P_{0i+1}} - \frac{1}{2RT_{i+1seal}\rho_{0i+1seal}}\right)P_{1i+1} + \frac{H_1}{C_r}\right] \quad (13)$$

Substituting Eqs. (12, 13) and linearized variables into Eq. (7) and neglecting the terms of order $\varepsilon^2$ and the higher, the first-order continuity equation for the *i*th cavity is reduced as

$$G_{10i}\left(\frac{\partial P_{1i}}{\partial t} + \frac{V_{0i}}{R_s}\frac{\partial P_{1i}}{\partial\theta} + \frac{P_{0i}}{R_s}\frac{\partial V_{1i}}{\partial\theta}\right) + G_{20i}P_{1i-1} + G_{30i}P_{1i} + G_{40i}P_{1i+1} = -G_{50i}\left(\frac{\partial H_1}{\partial t} + \frac{V_{0i}}{R_s}\frac{\partial H_1}{\partial\theta}\right), \quad (14)$$

where

$$G_{10i} = \frac{A_0}{RT_i},$$

$$G_{20i} = -0.5\dot{q}_0\left(\frac{1}{P_{0i-1} - P_{0i}} + \frac{1}{2RT_{iseal}\rho_{0iseal}}\right),$$

$$G_{30i} = -0.5\dot{q}_0\left(\frac{1}{P_{0i-1} - P_{0i}} + \frac{1}{P_{0i} - P_{0i+1}} + \frac{1}{2RT_{i+1}\rho_{0i+1seal}} - \frac{1}{2RT_i\rho_{0iseal}}\right),$$

$$G_{40i} = -0.5\dot{q}_0\left(\frac{1}{P_{0i} - P_{0i+1}} - \frac{1}{2RT_{i+1}\rho_{0i+1seal}}\right),$$

$$G_{50i} = \rho_{0i}L.$$

In like manner, considering Eq. (6) and substituting linearized variables into Eqs. (9, 10), we obtain

$$\tau_{s1i} = \frac{\tau_{s0i}}{\rho_{0i}}\frac{P_{1i}}{RT_i} + \frac{1.75\tau_{s0i}}{V_{0i}}V_{1i} - \frac{0.125\tau_{s0i}Dh_0}{\left(B + C_r\right)^2}H_1, \quad (15)$$

$$\tau_{r1i} = \frac{\tau_{r0i}}{\rho_{0i}}\frac{P_{1i}}{RT_i} + \frac{1.75\tau_{r0i}}{V_{0i} - R_s\omega}V_{1i} - \frac{0.125\tau_{s0i}Dh_0}{\left(B + C_r\right)^2}H_1. \quad (16)$$

In addition, substituting Eqs. (6), (12), (13), (15) and (16) together with linearized variables into Eq. (8) and neglecting the terms of order $\varepsilon^2$ and the higher, the first-order circumferential momentum equation for the *i*th cavity is reduced as

$$X_{10i}\left(\frac{\partial V_{1i}}{\partial t} + \frac{V_{0i}}{R_s}\frac{\partial V_{1i}}{\partial\theta}\right) + \frac{A_0}{R_s}\frac{\partial P_{1i}}{\partial\theta} + X_{20i}V_{1i} - q_0V_{1i-1} + X_{30i}P_{1i-1} + X_{40i}P_{1i} = X_{50i}H_1, \quad (17)$$

where

$$X_{10i} = \rho_{0i}A_0,$$

$$X_{20i} = \dot{q}_0 + \frac{1.75\tau_{s0i}a_sL}{V_{0i}} - \frac{1.75\tau_{r0i}a_rL}{V_{0i} - R_s\omega},$$

$$X_{30i} = 0.5\dot{q}_0\left(\frac{1}{P_{0i-1} - P_{0i}} + \frac{1}{2RT_{iseal}\rho_{0iseal}}\right)\left(V_{0i} - V_{0i-1}\right),$$

$$X_{40i} = \frac{L}{RT_i\rho_{0i}}\left(\tau_{s0i}a_s - \tau_{r0i}a_r\right) - 0.5\dot{q}_0\left(\frac{1}{P_{0i-1} - P_{0i}} - \frac{1}{2RT_{iseal}\rho_{0iseal}}\right)\left(V_{0i} - V_{0i-1}\right),$$

$$X_{50i} = -\frac{\dot{q}_0}{C_r}\left(V_{0i} - V_{0i-1}\right) + \frac{0.125Dh_0L}{\left(B + C_r\right)^2}\left(\tau_{s0i}a_s - \tau_{r0i}a_r\right).$$

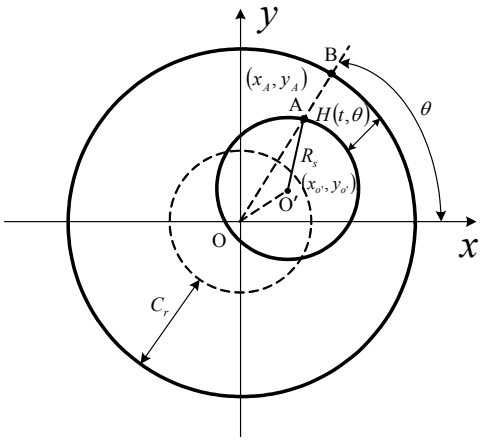


Fig. 3. Illustration of the orbital motion of the rotor.

Of note is that the coefficients embedded in Eqs. (14-17) are significantly different from those associated with the air leakage [15], which resulted from inclusion of thermal properties of the steam fluid in the model. Subsequently, the solution for nonlinear steam forcing on the rotor surface in the coverage of the cavity volume is drawn out with consideration of the steam properties. Due to the flow-structure interaction between the steam leakage and the rotor, the whirling orbit of the rotor cannot be assumed as preconditioned track [2-4, 8, 10 and 11]; actually, the position of the rotor center is a spatio-temporal variable $\left(x_{o'}(t), y_{o'}(t)\right)$ as shown in Fig. 3, which is iteratively calculated. The clearance function can be written as

$$H_1(t,\theta) = -(C_r + B)\left(\frac{x_{o'}(t)}{\sqrt{x_{o'}(t)^2 + y_{o'}(t)^2}}\cos\theta + \frac{y_{o'}(t)}{\sqrt{x_{o'}(t)^2 + y_{o'}(t)^2}}\sin\theta\right). \quad (18)$$

Eq. (18) is then rewritten as

$$H_1(t,\theta) = -(C_r + B)\mathrm{Re}\left\{e^{\eta(\theta-\beta)}\right\}, \quad (19)$$

in which $\beta = \arctan\left(\frac{y_{o'}(t)}{x_{o'}(t)}\right)$.

Substituting the forcing term $H_1(t,\theta)$ into Eqs. (14) and (17), we look for solutions of the form,

$$P_{1i}(t,\theta) = \mathrm{Re}\left\{P_i^+ e^{\eta(\theta+\beta)} + P_i^- e^{\eta(\theta-\beta)}\right\}, \quad (20)$$

$$V_{1i}(t,\theta) = \mathrm{Re}\left\{V_i^+ e^{\eta(\theta+\beta)} + V_i^- e^{\eta(\theta-\beta)}\right\}, \quad (21)$$

in which $P_i^+, P_i^-, V_i^+$ and $V_i^-$ in Eqs. (20-21) are constant complex coefficients ( $P_i^+ = p_i^+ + \eta p_i^{'+}$, $P_i^- = p_i^- + \eta p_i^{'-}$, $V_i^+ = v_i^+ + \eta v_i^{'+}$, $V_i^- = v_i^- + \eta v_i^{'-}$ ). Substituting Eqs. (19-21) into Eqs. (14) and (17) and eliminating the terms of $e^{\eta(\theta+\beta)}$ and $e^{\eta(\theta-\beta)}$ yields a set of four linearized equations for each cavity, which are dependent of *t*. The associated 12 unknowns included in these equations are $P_i^+, P_i^-, V_i^+$ and $V_i^-$ and their counterparts before and behind the *i*th cavity. The set of four equations is rearranged in the matrix form

$$\left[M_i^{-1}\right]\left\{Y_{i-1}\right\} + \left[M_i^{0}\right]\left\{Y_i\right\} + \left[M_i^{+1}\right]\left\{Y_{i+1}\right\} = \left\{E_i\right\}, \quad (22)$$

where

$$\left\{Y_i\right\} = \left[P_i^+, P_i^-, V_i^+, V_i^-\right]^T,$$

$$\left\{E_i\right\} = \left[0, -\eta G_{50i}(C_r + B)\left(\frac{d\beta}{dt} - \frac{V_{0i}}{R_s}\right), 0, -X_{50i}(C_r + B)\right]^T,$$

$$\left[M_i^{-1}\right] = \begin{bmatrix} G_{20i} & 0 & 0 & 0 \\ 0 & G_{20i} & 0 & 0 \\ X_{30i} & 0 & -q_0 & 0 \\ 0 & X_{30i} & 0 & -q_0 \end{bmatrix},$$

$$\left[M_i^{0}\right] = \begin{bmatrix} \eta G_{0i}\left(\frac{V_{0i}}{R_s} + \frac{d\beta}{dt}\right) + G_{30i} & 0 & \eta G_{30}\frac{p_{0i}RT_i}{R_s} & 0 \\ 0 & \eta G_{0i}\left(\frac{V_{0i}}{R_s} - \frac{d\beta}{dt}\right) + G_{30i} & 0 & \eta G_{30}\frac{\rho_{0i}RT}{R_s} \\ \eta\frac{A_0}{R_s} + X_{40i} & 0 & \eta X_{30i}\left(\frac{V_{0i}}{R_s} + \frac{d\beta}{dt}\right) + X_{20i} & 0 \\ 0 & \eta\frac{A_0}{R_s} + X_{40i} & 0 & \eta X_{30i}\left(\frac{V_{0i}}{R_s} - \frac{d\beta}{dt}\right) + X_{20i} \end{bmatrix},$$

$$\left[M_i^{+1}\right] = \begin{bmatrix} G_{40i} & 0 & 0 & 0 \\ 0 & G_{40i} & 0 & 0 \\ 0 & 0 & 0 & 0 \\ 0 & 0 & 0 & 0 \end{bmatrix}.$$

Here, the shaking frequency $\frac{d\beta}{dt}$ is defined as

$$\frac{d\beta}{dt} = \frac{\left[y_{o'}(t)\right]' x_{o'}(t) - \left[x_{o'}(t)\right]' y_{o'}(t)}{x_{o'}(t)^2},$$

which was simultaneously obtained by iterative calculation of the orbit of the whirling rotor.

For a labyrinth seal with $N$ cavities, a $4(N-1)\times 4(N-1)$ banded system of the linear Eq. (22) determines the $4(N-1)$ unknowns $P_i^+, P_i^-, V_i^+$ and $V_i^-$ for $i = 1, 2, \cdots, N-1$,

$$\begin{bmatrix} \bullet & \bullet & & & \\ M_{i-1}^{-1} & M_{i-1}^{0} & M_{i-1}^{+1} & & \\ & M_{i}^{-1} & M_{i}^{0} & M_{i}^{1} & \\ & & M_{i+1}^{-1} & M_{+1i}^{0} & M_{i+1}^{1} \\ & & & \bullet & \bullet \end{bmatrix} \begin{bmatrix} \bullet \\ Y_{i-1} \\ Y_{i} \\ Y_{i+1} \\ \bullet \end{bmatrix} = \begin{bmatrix} \bullet \\ E_{i-1} \\ E_{i} \\ E_{i+1} \\ \bullet \end{bmatrix}. \quad (23)$$

Hence, the set of Eq. (23) is readily solved by using the Gauss elimination method.

The total steam forcing $F(t)\big|_{ca}$ on the rotor in the coverage of the cavity volume is obtained by integrating the instantaneous pressure and shear stress along the circumferential direction. Consequently, the cavity reaction force components $F_y(t)\big|_{ca}$ and $F_x(t)\big|_{ca}$ derived from $F(t)\big|_{ca} = F_x(t)\big|_{ca} + \eta F_y(t)\big|_{ca}$ can be determined from Eq. (24), which will be used to analyze stabilization of the rotordynamics in Section 2.4.

$$\begin{cases} F_x(t)\big|_{ca} = -\varepsilon R_s L \sum_{i=1}^{N-1} \left\{ (Coef_1 + Coef_2)\cos\beta + (Coef_3 - Coef_4)\sin\beta \right\}, \\ F_y(t)\big|_{ca} = -\varepsilon R_s L \sum_{i=1}^{N-1} \left\{ (Coef_1 - Coef_2)\sin\beta - (Coef_3 + Coef_4)\cos\beta \right\} \end{cases} \quad (24)$$

where

$$\begin{cases} Coef_1 = p_i^- - p_i^{'-}\alpha_r \dfrac{\tau_{r0i}}{\rho_0 R T_i} - v_i^{'-}\alpha_r \dfrac{1.75\tau_{r0i}}{V_{0i} - \omega R_s} \\ Coef_2 = p_i^+ - p_i^{'+}\alpha_r \dfrac{\tau_{r0i}}{\rho_0 R T_i} - v_i^{'+}\alpha_r \dfrac{1.75\tau_{r0i}}{V_{0i} - \omega R_s} \\ Coef_3 = p_i^-\alpha_r \dfrac{\tau_{r0i}}{\rho_0 R T_i} + p_i^{'-} + v_i^-\alpha_r \dfrac{1.75\tau_{r0i}}{V_{0i} - \omega R_s} + \alpha_r \dfrac{0.125\tau_{r0i} D h_0}{(B + C_r)^2}(C_r + B) \\ Coef_4 = p_i^+\alpha_r \dfrac{\tau_{r0i}}{\rho_0 R T_i} + p_i^{'+} + v_i^+\alpha_r \dfrac{1.75\tau_{r0i}}{V_{0i} - \omega R_s} \end{cases}.$$

### *2.3 Steam forcing on the rotor surface in the coverage of the seal clearance*

The aforementioned deducing process of calculating the steam forcing on the rotor in the coverage of the cavity volume is performed by using perturbation analysis, which is reasonable because the local eccentricity ratio ($\varepsilon$) of the disturbed rotor is far less than 1.0. Here, the term $\varepsilon$ is determined to be $e/(C_r + B)$ and $e/C_r$ for the cavity volume and the seal clearance, respectively. In contrast to the radial height $(C_r + B)$ of the cavity, $C_r$ of the seal clearance is usually far small so that the steam forcing on the rotor in the coverage of the seal clearance may hold a strongly nonlinear relationship with the whirling rotor. Accordingly, the perturbation analysis cannot be readily adopted for the case of the steam leakage flow through the seal clearance. Hereafter, the Muzynska model [14] is used for accurate derivation of the steam forcing on the rotor surface in the coverage of the seal clearance.

By using the Muzynska model, the steam forcing on the rotor surface in the coverage of the seal clearance is formulated as below:

$$\begin{Bmatrix} F_x \\ F_y \end{Bmatrix}_{cl} = -\begin{bmatrix} K - \tau^2\omega^2 m_f & \tau\omega D \\ -\tau\omega D & K - \tau^2\omega^2 m_f \end{bmatrix} \begin{Bmatrix} X \\ Y \end{Bmatrix} - \begin{bmatrix} D & 2\tau\omega m_f \\ -2\tau\omega m_f & D \end{bmatrix} \begin{Bmatrix} \dot{X} \\ \dot{Y} \end{Bmatrix}, \\ - \begin{bmatrix} m_f & 0 \\ 0 & m_f \end{bmatrix} \begin{Bmatrix} \ddot{X} \\ \ddot{Y} \end{Bmatrix} \quad (25)$$

where $\tau$ is the ratio of the averaged circumferential velocity of the local leakage fluid to rotating speed $\omega$ of the rotor ($\tau$ is approximate to 0.5 [20]), $F_x$ and $F_y$ are the local steam forcing in the $X$ and $Y$ coordinates, respectively. In Eq. (25), $K$, $D$ and $m_f$ are equivalent stiffness, equivalent damping and equivalent mass, respectively; these are all nonlinear functions of the radial displacement $\left(x_{o'}(t), y_{o'}(t)\right)$ of the rotor [13,15 and 21],

$$\begin{aligned} & K = K_0\left(1-\varepsilon^2\right)^{-nn}, D = D_0\left(1-\varepsilon^2\right)^{-nn}, \quad nn = \frac{1}{2} \sim 3 \\ & \tau = \tau_0(1-\varepsilon)^b, \quad 0 < b < 1 \\ & m_f = \mu_2\mu_3 t_{cl}^2 \end{aligned}, \quad (26)$$

where the empirical parameter *nn* is set to 2 [21]. Detailed characteristics of $K_0$, $D_0$ and $m_f$ are referred to the works [13, 15 and 21].

Consequently, for a labyrinth seal with $N$ teeth, the total steam forcing on the rotor surface in the coverage of the seal clearances can be obtained by integrating the associated forces:

$$\begin{Bmatrix} F_x(t) \\ F_y(t) \end{Bmatrix}_{cl} = \begin{pmatrix} \sum_{i=1}^{N-1} F_{xi} \\ \sum_{i=1}^{N-1} F_{yi} \end{pmatrix} = \\ - \begin{bmatrix} \sum_{i=1}^{N} \left(K_i - \tau_i^2\omega^2 m_{fi}\right) & \sum_{i=1}^{N} \tau_i\omega D_i \\ -\sum_{i=1}^{N} \tau_i\omega D_i & \sum_{i=1}^{N} \left(K_i - \tau_i^2\omega^2 m_{fi}\right) \end{bmatrix} \begin{Bmatrix} X \\ Y \end{Bmatrix} \\ - \begin{bmatrix} \sum_{i=1}^{N} D_i & 2\sum_{i=1}^{N} \tau_i\omega m_{fi} \\ -2\sum_{i=1}^{N} \tau_i\omega m_{fi} & \sum_{i=1}^{N} D_i \end{bmatrix} \begin{Bmatrix} \dot{X} \\ \dot{Y} \end{Bmatrix} - \begin{bmatrix} \sum_{i=1}^{N} m_{fi} & 0 \\ 0 & \sum_{i=1}^{N} m_{fi} \end{bmatrix} \begin{Bmatrix} \ddot{X} \\ \ddot{Y} \end{Bmatrix} \quad (27)$$

### *2.4 Governing equation of rotor dynamics*

Recall that the aerodynamic forcing of the steam leakage on the rotor is closely related to the whirling motion of the rotor. The stabilization and response of the rotor system is characterized by the governing equation of rotordynamics,

$$\begin{bmatrix} m_r & 0 \\ 0 & m_r \end{bmatrix}\begin{pmatrix} \ddot{X} \\ \ddot{Y} \end{pmatrix}+\begin{bmatrix} D_e & 0 \\ 0 & D_e \end{bmatrix}\begin{pmatrix} \dot{X} \\ \dot{Y} \end{pmatrix}+\begin{bmatrix} K_e & 0 \\ 0 & K_e \end{bmatrix}\begin{pmatrix} X \\ Y \end{pmatrix} = \begin{pmatrix} F_x \\ F_y \end{pmatrix}\Big|_{cl}+\begin{pmatrix} F_x \\ F_y \end{pmatrix}\Big|_{ca}+\begin{pmatrix} F_x \\ F_y \end{pmatrix}\Big|_{br}-\begin{pmatrix} 0 \\ m_r g \end{pmatrix}, \tag{28}$$

in which the dimensionless parameters are defined as

$$\begin{aligned} &x = X/C_r, y = Y/C_r, \omega t_{cl} = \overline{T}, \\ &M = m_r + \sum m_f + \sum m_{fbr} \\ &\dot{X} = \dot{x}\omega C_r, \ddot{X} = \dot{x}\omega^2 C_r \\ &\dot{Y} = \dot{y}\omega C_r, \ddot{Y} = \ddot{y}\omega^2 C_r \end{aligned}. \tag{29}$$

It is of note that in the present study the nonlinear oil film forces $F_x(t)\big|_{br}$ and $F_y(t)\big|_{br}$ exerted by the annual journal bearings are also calculated by using the Muzynska model reduced in section 2.3.

Substituting Eq. (29) into Eq. (28) and leaving the total steam forcing to the left hand of the equation leads to the following set of governing equations:

$$\begin{bmatrix} 1 & 0 \\ 0 & 1 \end{bmatrix}\begin{pmatrix} \ddot{x} \\ \ddot{y} \end{pmatrix}+\begin{bmatrix} D_1 & D_2 \\ -D_2 & D_1 \end{bmatrix}\begin{pmatrix} \dot{x} \\ \dot{y} \end{pmatrix}+\begin{bmatrix} K_1 & K_2 \\ -K_2 & K_1 \end{bmatrix}\begin{pmatrix} x \\ y \end{pmatrix}=\begin{pmatrix} G_1 \\ G_2 \end{pmatrix}, \tag{30}$$

where

$$\begin{aligned} K_1 &= \frac{K_e + \left(K_{br} - \tau_{br}^2\omega^2 m_{fbr}\right) + \sum_{i=1}^{N}\left(K_i - \tau_i^2\omega^2 m_{fi}\right)}{M\omega^2}, \\ K_2 &= \frac{\tau_{br}D_{br} + \sum_{i=1}^{N}\tau_i D_i}{M\omega}, \\ D_1 &= \frac{D_e + D_{br} + \sum_{i=1}^{N} D_i}{M\omega}, \\ D_2 &= \frac{2\tau_{br}D_{br} + 2\sum_{i=1}^{N}\tau_i D_i}{M}, \end{aligned} \tag{31}$$

$$G_1 = \frac{F_x(t)\big|_{ca}}{MC_r\omega^2},$$

$$G_2 = \frac{F_y(t)\big|_{ca} - m_r g}{MC_r\omega^2}.$$

In calculation, Eq. (30) is solved by using the fourth-order Runge-Kutta method to obtain the orbit of the whirling rotor.

### *2.5 Stability analysis*

Stability analysis of the whirling rotor, which is under the considerable influence of steam leakage through the interlocking seal, is subsequently carried out by using Liapunov's first theorem. Toward this end, Eq. (26) is rearranged as

$$\begin{pmatrix} \ddot{x} \\ \ddot{y} \\ \dot{x} \\ \dot{y} \end{pmatrix}+\begin{bmatrix} -D_1 & -D_2 & -K_1 & -K_2 \\ D_2 & -D_1 & K_2 & -K_1 \\ 1 & 0 & 0 & 0 \\ 0 & 1 & 0 & 0 \end{bmatrix}\begin{pmatrix} \dot{x} \\ \dot{y} \\ x \\ y \end{pmatrix}+\begin{pmatrix} G_1 \\ G_2 \\ 0 \\ 0 \end{pmatrix}=\begin{pmatrix} f_1(\dot{x},\dot{y},x,y,\omega) \\ f_2(\dot{x},\dot{y},x,y,\omega) \\ f_3(\dot{x},\dot{y},x,y,\omega) \\ f_4(\dot{x},\dot{y},x,y,\omega) \end{pmatrix}. \tag{32}$$

The stability of the rotor-seal system at the equilibrium point $(x_0, y_0)$ is determined by the real parts of all eigenvalues obtained from the Jacobi matrix $J = Df\big|_{(x_0,y_0)}$. The threshold of instability is reached when the real part of one eigenvalue changes from negative to positive.

## 3. Results and discussion

Now we turn to the applicability of the perturbation analysis and the Muzynska model in calculations of the steam forcing in the coverage of the cavity volume and the seal clearance, respectively. The orbital motions of the rotor at various operating conditions (Table 2), which are adopted in the 1000 MW supercritical and 300 MW subcritical power units, were calculated in the present study. The inlet circumferential velocity $V_0$ was fixed to 0 [21]. For the conditions $n = 1.30$ and $n = 1.53$, $N$=16, $R_s$=50, the orbital motions of the rotor at different rotating speeds $\omega = 5000$, 6000, 7000, 8000, 9000 and 10000 *rpm* are shown in Fig. 4. As seen from Fig. 4, the excursion of the whirling orbit from the equilibrium point starts at $\omega = 6000$ *rpm*; furthermore, the amplitude of the deviation increases with the increasing rotor speed. The accretion level of the local eccentricity $\varepsilon$

Table 2. Operating conditions of the interlocking seal.

| | |
|---|---|
| Inlet and Outlet Pressure(MPa) | (17.6,13.5($n$=1.30)): 1000 MW<br>(11.3,7.4($n$=1.53)): 300 MW<br>(11.3,8.7(n=1.30)): for comparison |
| Inlet and Outlet Temperature($^0$C): | (530.8,513.5): 1000 MW<br>(479.8, 460.5): 300 MW<br>(530.8,513.5): for comparison |
| Rotating speed: $\omega$ (rpm) | 4000,5000,6000,7000,8000,9000,10000 |
| Inlet circumferential velocity: $V_0$ (m/s) | 0 |
| Tooth number: $N$ | 16,20,24,26,32,36,40,44 |
| Radius of the rotor: $R_s$ (mm) | 50 |

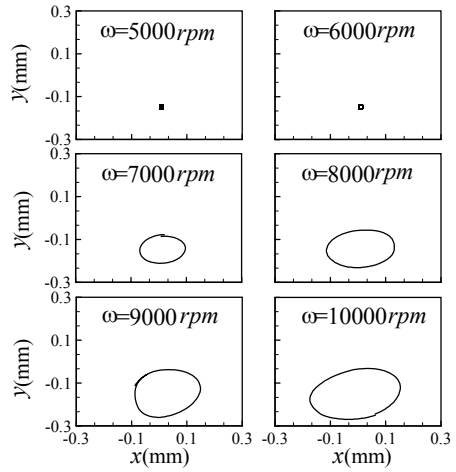


(a) $n$=1.53

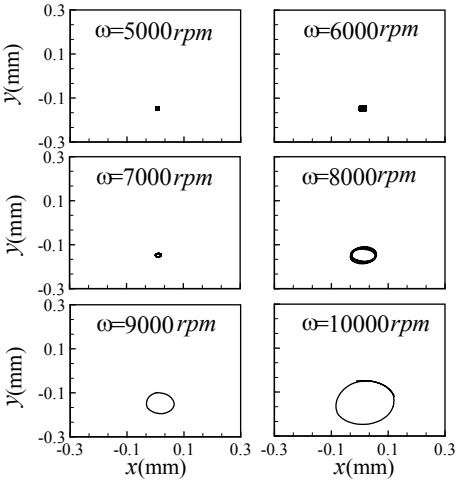


(b) $n$=1.30

Fig. 4. The orbital motion of the rotor at different rotating speeds: (1) $\omega = 5000$ *rpm*, (2) $\omega = 6000$ *rpm*, (3) $\omega = 7000$ *rpm*, (4) $\omega = 8000$ *rpm*,(5) $\omega = 9000$ *rpm*, (6) $\omega = 10000$ *rpm.*

for the cavity volume is far less than that for the seal clearance. The numerical investigation exhibits that the local eccentricity $\varepsilon$ calculated is far less than 0.01 for both the cavity and the seal clearance at $\omega = 5000$ and 6000 *rpm*, indicating a weak nonlinear relationship between the whirling rotor and the leakage flow through the labyrinth seal. However, the deviation $\varepsilon$ of the rotor from the equilibrium position under the conditions of rotating speed over 6000 *rpm* increases beyond 0.1 for the seal clearance, while $\varepsilon$ is still less than 0.02 in the coverage of the cavity volume. This reflects that the steam forcing of the leakage flow through the seal clearance holds a strongly nonlinear relationship with the whirling rotor.

With the increase in the steam pressure and the decrease in the seal clearance, steam-excited rotor vibration becomes a crucial problem in system design or operation. Accordingly, further understanding of the influence of steam leakage on the whirling rotor is gained through comparing the orbital motions under the pressure ratio $n = 1.30$ and $n = 1.53$ while the rotating speed of the rotor ($N$=16, $R_s$=50 mm) is kept at $\omega = 4000$, 6000, 8000 and 10000 *rpm*. The orbital motions of the rotor at $n$ = 1.30 and 1.53 are shown in Fig. 5. Inspection of Fig. 5 demonstrates that the orbital magnitude of the whirling rotor is increased with the increasing the pressure ratio, which is attributed to the intensified steam forcing on the rotor surface. Furthermore, the increase of the rotating speed results in the accretion of the orbital magnitude of the whirling rotor. This is induced by the increment of the destabilizing tangential forcing on the rotor due to intensification of the tangential compensation flow in the seals when increasing the rotating speed [22]. Subsequently, the magnification development of the deviation of the rotor from the equilibrium position with the increase of the rotating speed is shown in Fig. 6, in which the numerical results at the conditions of $n$ = 1.30 and 1.53 are provided for a detailed comparison. The orbital magnitude of the whirling rotor is increased in going from $\omega = 6200$ to 6600 rpm, indicating the destabilized influence of the rotating speed on the rotor. This is due to the fact that the tangential compensation flow has a considerable effect on the magnitude of the steam forcing on the rotor with the increase of the rotating speed and the local eccentricity. Furthermore, a comparison of the orbital motions of the rotor at the conditions of $n$ = 1.30 and 1.53 shows that the orbital magnitude at the latter condition is larger, which corresponds to destabilization of

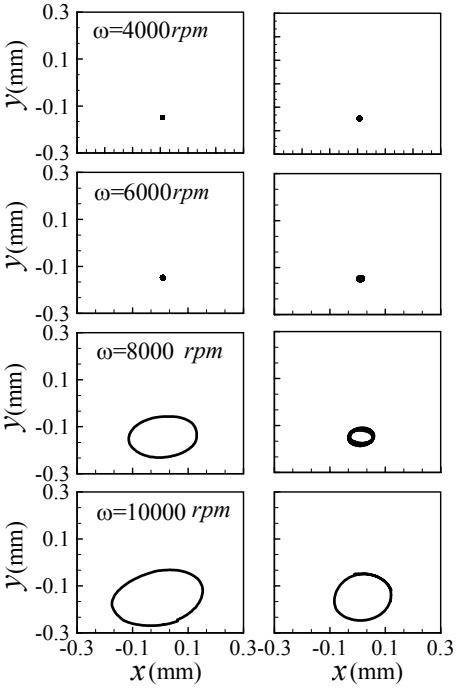


Fig. 5. Comparison of the orbital motion at different rotor speed under the conditions of (a) $n$=1.53 and (b) $n$=1.30.

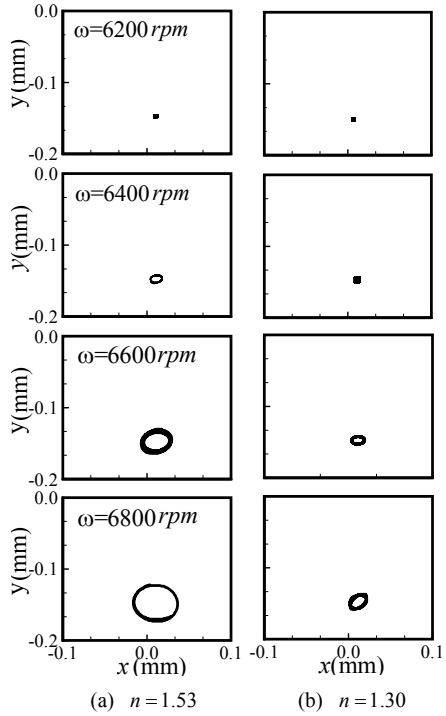


Fig. 6. The orbital motion of the rotor at the destabilization point varying different rotating speeds (a) $n$=1.53, (b) $n$=1.30.

the rotating rotor due to the intensified influence of the steam leakage through the interlocking seal.

Subsequently, stability analysis of the rotating rotor subject to the steam leakage is performed to illuminate the destabilizing effect of the steam forcing on the rotor. Table 3 contains the numerical results at $N$=16, $R_s$=50 mm by using Liapunov's first method. A general observation of the data in Table 3 indicates that the real part of one eigenvalue crosses the zero line from the negative around 6000 *rpm* and increases with the increase of the rotating speed for both conditions at $n$ = 1.30 and 1.53. This illustrates that the destabilization speed of the rotor is intensified with increasing the rotor speed under the influence of the steam leakage, which is towel consistent with the aforementioned calculation of the orbital motions shown in Fig. 4. Additionally, the destabilization speed is numerically investigated by using Liapunov's first method with increasing the rotating speed from 6000 *rpm*. According to the results of the eigenvalues of the Jacobi matrix shown in Table 4, the destabilization speed of the rotor under the influence of the steam flow at the condition of $n$ = 1.53 is 6200 *rpm*, while it is increased to 6400 *rpm* at $n$ = 1.30. This convincingly demonstrates the destabilization influence of the steam leakage on the rotating rotor. In addition, the pressure ratio of the labyrinth seal should be taken into careful consideration.

Geometrical influence of the rotor-seal system on stability of the rotor is obtained by varying the number of seals ($N$) while the pressure ratio is kept at $n$ = 1.30 and 1.53. Fig. 7 shows the destabilization speed of the rotating rotor with different number of seal teeth. It is clear that the destabilization speed is linearly reduced with increasing the number of the seal teeth. Furthermore, the destabilization speed at $n$ = 1.30 is less than that at $n$ = 1.53. In addition, the calculation of the mass flow rate of the labyrinth seal at the conditions of $n$ = 1.30 and 1.53 is performed in the present study by varying the number of seals ($N$) and shown in Fig. 8. It shows that the mass flow rate decreases with increasing the number of seals. Furthermore, the mass flow rate at $n$ = 1.53 is less than that at $n$ = 1.30 due to the higher inlet steam parameters in the latter case. The orbital motions at different conditions of the inlet and outlet pressure, e.g., (17.6 Mpa, 13.5 Mpa) and (11.3 Mpa, 8.7 Mpa), are calculated and shown in Fig. 9. The orbital magnitude of the whirling rotor increases with increasing the rotor speed. Of the two conditions, the orbital magnitude of

Table 3. Eigenvalues of Jacobi matrix at different rotating speeds of the rotor.

(a) $n$=1.53

| Rotating speed (rpm) | $X_1$ | $X_2$ | $X_3$ | $X_4$ |
|---|---|---|---|---|
| 4000 | -0.013+0.876i | -0.013-0.876i | -0.058+0.864i | -0.058-0.864i |
| 5000 | -0.006+0.701i | -0.006-0.701i | -0.048+0.690i | -0.048-0.690i |
| 6000 | -0.001+0.584i | -0.001-0.584i | -0.042+0.574i | -0.042-0.574i |
| 7000 | 0.002+0.501i | 0.002-0.501i | -0.042+0.492i | -0.042-0.492i |
| 8000 | 0.007+0.437i | 0.007-0.437i | -0.027+0.427i | -0.027-0.427i |
| 9000 | 0.010+0.388i | 0.010-0.388i | -0.027+0.380i | -0.027-0.380i |
| 10000 | 0.015+0.350i | 0.015-0.350i | -0.031+0.343i | -0.031-0.343i |

(b) $n$=1.30

| Rotating speed (rpm) | $X_1$ | $X_2$ | $X_3$ | $X_4$ |
|---|---|---|---|---|
| 4000 | -0.013+0.876i | -0.013-0.876i | -0.058+0.864i | -0.058-0.864i |
| 5000 | -0.006+0.701i | -0.006-0.701i | -0.049+0.690i | -0.049-0.690i |
| 6000 | -0.001+0.584i | -0.001-0.584i | -0.042+0.574i | -0.042-0.574i |
| 7000 | 0.001+0.500i | 0.001-0.500i | -0.040+0.492i | -0.040-0.492i |
| 8000 | 0.005+0.438i | 0.005-0.438i | -0.045+0.431i | -0.045-0.431i |
| 9000 | 0.008+0.388i | 0.008-0.388i | -0.027+0.380i | -0.027-0.380i |
| 10000 | 0.012+0.351i | 0.012-0.351i | -0.042+0.344i | -0.042-0.344i |

Table 4. Eigenvalues of Jacobi matrix at destabilization rotating speeds of the rotor.

(a) $n$=1.53

| Rotating speed (rpm) | $X_1$ | $X_2$ | $X_3$ | $X_4$ |
|---|---|---|---|---|
| 6000 | -0.001+0.584i | -0.001-0.584i | -0.043+0.574i | -0.043-0.574i |
| 6200 | 0.000+0.565i | 0.000-0.565i | -0.042+0.556i | -0.042-0.556i |
| 6400 | 0.001+0.547i | 0.001-0.547i | -0.041+0.538i | -0.041-0.538i |
| 6600 | 0.001+0.531i | 0.001-0.531i | -0.044+0.522i | -0.044-0.522i |

(b) $n$=1.30

| Rotating speed (rpm) | $X_1$ | $X_2$ | $X_3$ | $X_4$ |
|---|---|---|---|---|
| 6000 | -0.001+0.584i | -0.001-0.584i | -0.042+0.574i | -0.042-0.574i |
| 6200 | -0.001+0.565i | -0.001-0.565i | -0.042+0.556i | -0.042-0.556i |
| 6400 | 0.000+0.547i | 0.000+0.547i | -0.040+0.538i | -0.040-0.538i |
| 6600 | 0.001+0.531i | 0.001-0.531i | -0.039+0.522i | -0.039-0.522i |

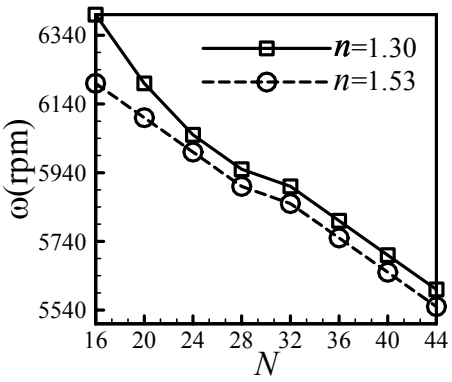


Fig. 7. Dependence of the destabilization speed on the number of teeth ($n$ = 1.30 and $n$ = 1.53).

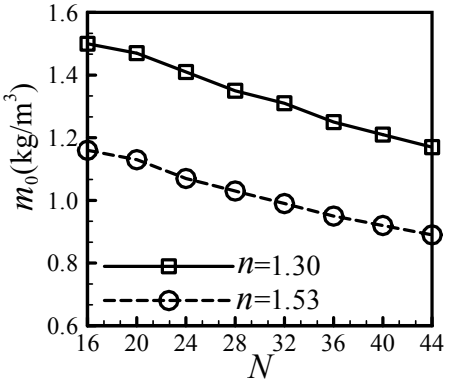


Fig. 8. Dependence of the leakage mass flow rate on the number of teeth ($n$ = 1.30 and $n$ = 1.53).

Table 5. Eigenvalues of Jacobi matrix at different rotating speeds of the rotor and at same pressure ratio.

(a) (11.3, 8.7($n$=1.30))

| Rotating speed (rpm) | $X_1$ | $X_2$ | $X_3$ | $X_4$ |
|---|---|---|---|---|
| 4000 | -0.013+0.876i | -0.013-0.876i | -0.058+0.864i | -0.058-0.864i |
| 6000 | -0.001+0.584i | -0.001-0.584i | -0.041+0.574i | -0.041-0.574i |
| 8000 | 0.005+0.437i | 0.005-0.437i | -0.028+0.428i | -0.028-0.428i |
| 10000 | 0.015+0.351i | 0.015-0.351i | -0.043+0.345i | -0.043-0.345i |

(b) (17.6, 13.5($n$=1.30))

| Rotating speed (rpm) | $X_1$ | $X_2$ | $X_3$ | $X_4$ |
|---|---|---|---|---|
| 4000 | -0.013+0.876i | -0.013-0.876i | -0.058+0.864i | -0.058-0.864i |
| 6000 | -0.001+0.584i | -0.001-0.584i | -0.042+0.574i | -0.042-0.574i |
| 8000 | 0.001+0.547i | 0.001-0.547i | -0.041+0.538i | -0.041-0.538i |
| 10000 | 0.012+0.351i | 0.012-0.351i | -0.042+0.344i | -0.042-0.344i |

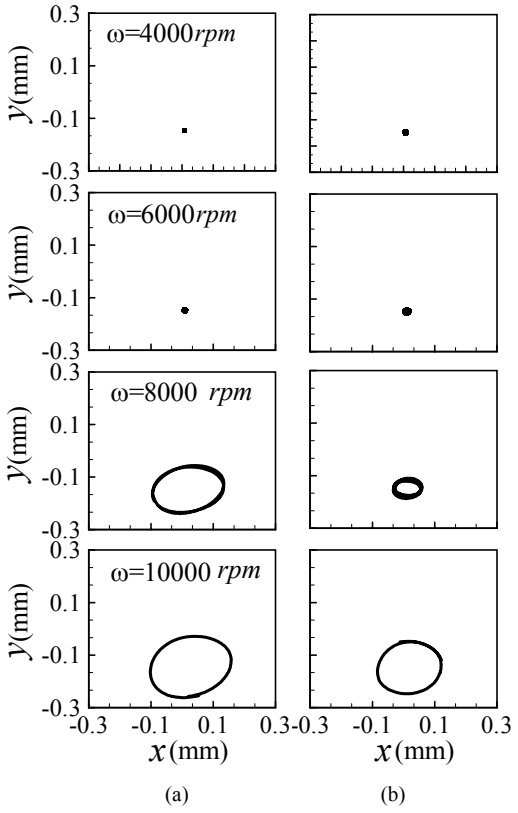


Fig. 9. The orbital motion of the rotor at the destabilization point varying different rotating speeds at the same pressure ratio but the different inlet pressure (a) (11.3,8.7($n$=1.30)), (b) (17.6,13.5($n$=1.30)).

the whirling rotor with high inlet and outlet pressure is larger. Further stability analysis on the orbital motion of the rotor was performed by using Liapunov's first method. The data displayed in Table 5 shows that the destabilization of the orbital motion of the rotor is worsened at higher inlet and outlet pressure.

## 4. Conclusion

A nonlinear model of flow-structure interaction between the steam leakage through the labyrinth seal and the rotor is presented. The rotor-seal system was modeled as a Jeffcott rotor subject to steam forcing induced by the leakage flow. Particular attention was placed at thermal properties of the steam fluid specified by IAPWS-IF97. To see influence of the steam fluid on the whirling rotor, two sets of thermal parameters of the steam fluid, temperature and pressure drop in each seal cavity, were selected from the typical 1000 MW supercritical and 300 MW subcritical power units in China. The steam forcing associated with the seal clearance, which is strongly coupled with the whirling rotor, was obtained by using the Muzynska mode. A perturbation analysis was employed to delineate the spatio-temporal variation of the pressure and the shear stress on the rotor. The unsteady steam forcing integrated at all seal clearances and cavity volumes was incorporated into governing equation of the rotordynamics, which was then solved by using the fourth-order Runge-Kutta method for further nonlinear analysis. Stability of the rotating rotor was inspected by employing Liapunov's first

method. The orbital motion of the rotor was analyzed in terms of the pressure ratio and the rotating speed. The orbital magnitude of the rotor with steam leakage at high pressure ratio was shown to be larger than that at low pressure ratio, indicating the intensified influence of the steam leakage on stabilization of the rotating rotor. In addition, stability analysis by using Liapunov's first method convincingly demonstrated that the destabilization speed of the rotor was reduced due to aerodynamic forcing of the steam leakage. The nonlinear model of the flow-structure interaction between the steam leakage and the rotor would be helpful to designers of the supercritical steam turbines.

## Acknowledgment

This work was supported by grants from the Chinese Ministry of Education major program (No.309012), national Natural Science Foundation of China (No.10732060) and Natural Science Foundation of Shanghai City (No. 07ZR14049).

## Nomenclature

$A_n$ : Unsteady cross-sectional area of the cavity ($m^2$)
$A_0$ : Steady annular flow area ($m^2$)
$B$ : Tooth height (m)
$C_0$ : Orifice contraction coefficient
$C_1$ : Kinetic energy carry-over coefficient
$C_r$ : Steady radial clearance (m)
$Dh_0$ : Steady hydraulic diameter of the cross-sectional area of the cavity (m)
$Dh$ : Unsteady hydraulic diameter of the cross-sectional area of the cavity (m)
$D_e$ : Damping coefficient of the rotor (N s/m)
$D_i$ : Equivalent damping of steam flow at the *i*th seal clearance (N s/m)
$D_{br}$ : Equivalent damping of oil film in the journal bearings (N s/m)
$e$ : Displacement of the rotor from the central position (m)
$F(t)\big|_{ca}$ : Total steam reaction force in the cavities (N)
$F_x(t)\big|_{br}$ : Journal bearing reaction force component in the $X$ direction(N)
$F_y(t)\big|_{br}$ : Journal bearing reaction force component in the $Y$ direction(N)
$F_x(t)\big|_{ca}$ : Cavity reaction force component in the $X$ direction (N)
$F_y(t)\big|_{ca}$ : Cavity reaction force component in the $Y$ direction (N)
$F_x(t)\big|_{cl}$ : Seal clearance reaction force component in the $X$ direction (N)
$F_y(t)\big|_{cl}$ : Seal clearance reaction force component in the $Y$ direction (N)
$h_{0iseal}$, $h_{iseal}$ : Steady and unsteady local enthalpy at the *i*th clearance (J/Kg)
$h_0$ : Stagnant enthalpy (J/Kg)
$H$ : Unsteady labyrinth seal radial clearance (m)
$H_1(t,\theta)$ : Perturbation clearance (m)
$L$ : Pitch of the cavity (m)
$m_0$ : Leakage flow through the labyrinth seal (kg/s)
$m_r$ : Mass of the rotor (kg)
$m_{fi}$ : Equivalent mass of steam flow at the *i*th seal clearance (kg)
$m_{fbr}$ : Equivalent mass of oil film in the journal bearings (kg)
$N$ : Tooth number
$n$ : Pressure ratio of the labyrinth seal
$P_{0iseal}$, $P_{iseal}$ : Steady and unsteady pressure at the *i*th seal clearance (Pa)
$P_{0i}$ $P_i$ : Steady and unsteady pressure in the *i*th cavity (Pa)
$P_{1i}(t,\theta)$ : Perturbation pressure in the *i*th cavity (Pa)
$\dot{q}_{0i}$, $\dot{q}_i$ : Steady and unsteady leakage rate per unit length (kg/s m)
$\dot{q}_{1i}(t,\theta)$ : Perturbation leakage flow rate per unit length (kg/s m)
$R_s$ : Rotor radius (m)
$T_i$ : Temperature at the *i*th cavity (K)
$T_{iseal}$ : Temperature at the *i*th orifice (K)
$U_{0iseal}$ : Steady axial veclity at the *i*th seal clearance (m/s)
$V_{0i}$ : Steady circumferential velocities at the *i*th cavity (m/s)
$V_i$ : Unsteady circumferential velocities at the *i*th cavity (m/s)
$V_{1i}(t,\theta)$ : Perturbation pressure at the *i*th cavity (m/s)
$W$ : Width of tooth (m)
$(x_{o'}(t), y_{o'}(t))$ : $x$ and $y$ coordinates of the whirling rotor (m)

### *Greek symbols*

$\alpha_r$ : Dimensionless shear stress length at the rotor wall
$\alpha_s$ : Dimensionless shear stress length at the stator wall

$\varepsilon$ : Eccentricity ratio
$\eta$ : Imaginary number
$\theta$ : Azimuthal position
$\rho_{0iseal}$ , $\rho_{iseal}$ : Steady and unsteady gas density at the *i*th clearance (kg/m$^3$)
$\rho_{1iseal}(\theta,t)$ : Perturbation gas density at the *i*th clearance (kg/m$^3$)
$\rho_{0i}$ , $\rho_i$ : Perturbation gas density at the *i*th clearance (kg/m$^3$)
$\rho_1(\theta,t)$ : Perturbation gas density of the *i*th cavity (kg/m$^3$)
$\tau_{br}$ : Ratio of circumferential velocity of the oil film in the journal bearings to the rotor surface speed
$\tau_i$ : Ratio of circumferential velocity of the steam flow at the *i*th seal clearance to the rotor surface speed
$\tau_{r0i}$ , $\tau_{ri}$ : Steady and unsteady shear stresses at the rotor wall (N/m$^2$)
$\tau_{r1i}(t,\theta)$ : Perturbation shear stresses at the rotor wall (N/m$^2$)
$\tau_{s0i}$ , $\tau_{si}$ : Steady and unsteady shear stresses at the stator wall (N/m$^2$)
$\tau_{s1i}(t,\theta)$ : Perturbation shear stresses at the stator wall (N/m$^2$)
$\omega$ : Rotating speed of the rotor (rpm)

***Subscriptions***

*Cl* : Clearance of the labyrinth seal
*ca* : Cavity volume of the labyrinth seal
*br* : Journal bearing

## Reference


[1] D. W. Childs and J. K. Scharrer, Theory versus experiment for the rotordynamic coefficients of labyrinth gas seals: part II-a comparison to experiment, *Rotating Machinery Dynamics*, *Vol.2*, *Proceedings from ASME Conference on Mechanical Vibration and Noise*, Boston, MA. (1987) 427-434.

[2] E. Dursun and J. Y. Kazakia, Air flow in cavities of labyrinth seals, *International Journal of Engineering Science*, 33 (1995) 2309-2326.

[3] E. Dursun, Rotordynamic coefficients in stepped labyrinth seals, *Computer Methods in Applied Mechanics and Engineering*, 191 (2002) 3127-3135.

[4] U. Yucel, Calculation of leakage and dynamic coefficients of stepped labyrinth gas seals, *Applied Mathematics and Computation*, 152 (2004) 521-533.

[5] A. G. Kostyuk, A theoretical analysis of the aerodynamic forces in the labyrinth glands of turbomachines, *Teploenergetica*, 19 (1972) 29-33.

[6] T. Iwatsubo, Evaluation of instability forces of labyrinth seals in turbines or compressors, rotordynamic instability problems in high-performance turbomachinery, *NASA CP*, 2133 (1980) 139-167.

[7] M. C. Rosen, *University of Virginia Report #UVA/643092/MAE86/346* (1986).

[8] U. Yucel and J. Y. Kazakia, Analytical prediction techniques for axisymmetric flow in gas labyrinth seals, *ASME Journal of Engineering for Gas Turbines and Power*, 123 (2001) 255-257.

[9] G. Kleynhans, A two-control-volume bulk-flow rotordynamic analysis for smooth-rotor/honeycomb-stator gas annular seal, *Dissertation*, Mechanical Engineering, Texas A&M University, (1996) 55-57.

[10] Y. Z. Liu, W. Z. Wang, H. P. Chen, Q. Ge and Y. Yuan, Influence of leakage flow through labyrinth seals on rotordynamics: numerical calculations and experimental measurements, *Archive of Applied Mechanics*, 77 (2007) 601-603.

[11] W. Z. Wang, Y. Z. Liu, H. P. Chen and P. N. Jiang, Computation of rotordynamic coefficients associated with leakage steam flow through labyrinth seal, *Archive of Applied Mechanics*, 77 (2007) 589-595.

[12] J. Hua, S. Swaddiwudhipong, Z. S. Liu and Q. Y. Xu, numerical analysis of nonlinear rotor-seal system, *Journal of Sound and Vibration*, 283 (2005) 525-542.

[13] M. Cheng, G. Meng and J. P. Jin, Non-linear dynamics of a rotor-bearing-seal system, *Archive of Applied Mechanics*, 76 (2006) 215-227.

[14] A. Muzynska, Whirl and whip-rotor/bearing stability problems, *Journal of Sound and Vibration*, 110 (1986) 443-462.

[15] W. Z. Wang, Y. Z. Liu, G. Meng and P. N. Jiang, Nonlinear analysis of orbital motion of the rotor subject to leakage air flow through an interlocking seal, *Journal of Fluids and Structures*, 25(2) (2009).

[16] W. J. Kearton, *Steam Turbine Theory and Practice*, Pitman, London (1958).

[17] *The International Association for the Properties of Water and Steam: Release on the IAPWS Industrial Formulation 1997 for the Thermodynamic Properties of Water and Steam*, Erlangen, Germany September (1997).

[18] K. J. Salisbury, *Steam Turbine and Their Cycles*, Robert E. Krieger Publishing Company, Huntington, New York (1974).

[19] M. I. Gurevich, *Theory of Jets in an Ideal Fluid*, Pergamon Press, Oxford, (1966).
[20] A. Muzynska and D. E Bently, Frequency-swept rotating input perturbation techniques and identification of the fluid force models in rotor/bearing/seal systems and fluid handling machines, *Journal of Sound and Vibration*, 143 (1990) 103-124.
[21] S. T. Li and Q. Y, Xu, Stability and bifurcation of unbalance rotor/labyrinth seal system, *Applied Mathematics and Mechanics*, 24 (2003) 1290-1301.
[22] J. P. Thomas, *Investigation into the flow-induced instability of high pressure rotors of large steam turbines*, University of Pennsylvania, (1988).

**Wei Zhe WANG**, Post-doc, School of Mechanical Engineering, Shanghai Jiao Tong University, 800 Dongchuan road, Shanghai 200240, China. Email: wangwz0214@sjtu.edu.cn.
Research interests: Flow-Induced Vibration in Turbomachinery; Advanced Sealing Technology; Advanced Computational Fluid Dynamics; Nonlinear Flow-Structure Analysis.

**Ying Zheng LIU**, Dr. Eng., Professor, School of Mechanical Engineering, Shanghai Jiao Tong University, 800 Dongchuan road, Shanghai 200240, China. Email: yzliu@sjtu.edu.cn.
Research interests: Flow Control; Separated Flow; Flow and Structure Analysis of Thermal System.